

Improving extractions of $|V_{cb}|$ and m_b from the hadronic invariant mass moments of semileptonic inclusive B decay

Michael Trott*

Department of Physics, University of Toronto, 60 St. George Street, Toronto, Ontario, Canada, M5S 1A7
(Received 17 March 2004; published 5 October 2004)

We calculate the hadronic tensor for inclusive semileptonic $B \rightarrow X_c \ell \bar{\nu}$ decay to $\mathcal{O}(\alpha_s)$. This allows $\mathcal{O}(\alpha_s \Lambda_{\text{QCD}}/m_b)$ corrections to hadronic invariant mass observables to be directly evaluated with experimentally required cuts on phase space. Several moments of phenomenological interest are presented to order $\mathcal{O}(\alpha_s \Lambda_{\text{QCD}}/m_b)$ and $\mathcal{O}(\Lambda_{\text{QCD}}^3/m_b^3)$, allowing a consistent extraction of the heavy quark effective theory parameters up to $\mathcal{O}(\Lambda_{\text{QCD}}^3/m_b^3)$ and the b quark mass with theoretical error ~ 50 MeV. The hadronic invariant mass spectrum is examined with a general moment to obtain observables that test the theoretical error estimate assigned to these parameters; in particular, fractional moments that directly test the operator product expansion for inconsistencies in the hadronic invariant mass spectrum are reported. The $m_b \Lambda_{\text{QCD}}/m_c^2$ expansion present for fractional moments of the hadronic invariant mass spectrum is discussed and shown to introduce a numerically suppressed uncertainty of $\mathcal{O}(m_b^4 \Lambda_{\text{QCD}}^4/m_c^8)$.

DOI: 10.1103/PhysRevD.70.073003

PACS numbers: 12.15.Hh, 12.38.Bx, 12.39.Hg, 13.20.He

I. INTRODUCTION

Inclusive semileptonic $B \rightarrow X_c \ell \bar{\nu}$ decay offers an opportunity to measure the Cabibbo-Kobayashi-Maskawa (CKM) parameter $|V_{cb}|$ and the bottom quark mass [1–9]. Measurements of these parameters are crucial to the B factory program of overconstraining the CKM sector of the standard model [10]. Experimental studies of moments of the differential decay spectrum of $B \rightarrow X_c \ell \bar{\nu}$ combined with a measurement of the total inclusive decay rate are useful in extracting these parameters, as these observables can be measured cleanly by experiment, and calculated from QCD without model dependence using an operator product expansion (OPE).

The OPE is an expansion in powers of the ratio Λ_{QCD}/m_b , where the terms in this expansion are parametrized using heavy quark effective theory (HQET). The OPE demonstrates that in the $m_b \rightarrow \infty$ limit, inclusive B meson decay spectra are equal to b quark decay spectra. To extract m_b and $|V_{cb}|$ from the inclusive decay spectrum with high precision, one needs to accurately know the relevant matrix elements of terms in the OPE that the spectrum depends upon. Extensive theoretical effort has been devoted to calculating the decay rates and moments of various spectra, to test HQET by the extractions of these nonperturbative parameters from different spectra, and to obtain $|V_{cb}|$ and a precise value for the b quark mass.

Experimental results have been reported by the BABAR, CLEO and DELPHI Collaborations measuring various B meson decay spectra and moments [11–16]. Recent analysis of this data [17,18] finds $|V_{cb}| = (40.8 \pm 0.9) \times 10^{-3}$ and $m_b^{1S} = 4.74 \pm 0.10$ GeV, where the experimental uncertainties dominate the extraction. As the

experimental errors are expected to decrease in the near future, it is appropriate to reexamine the theoretical error assigned in this extraction. The largest contributions to the theoretical uncertainties introduced in these fits come from the estimated size of the $\mathcal{O}(\alpha_s \Lambda_{\text{QCD}}/m_b)$ corrections with a lepton energy cut, the $\mathcal{O}(\alpha_s \Lambda_{\text{QCD}}^2/m_b^2)$ terms, and the $\mathcal{O}(\Lambda_{\text{QCD}}^4/m_b^2 m_c^2)$ terms introduced due to the HQET expansion employed for m_c [19].

In past calculations, the lepton energy cut dependence of the $\mathcal{O}(\alpha_s \Lambda_{\text{QCD}}/m_b)$ terms was not calculated, and these terms were treated as a source of error in the determination of m_b and $|V_{cb}|$. In this paper, we improve upon past results by calculating the lepton energy cut dependence of the $\mathcal{O}(\alpha_s \Lambda_{\text{QCD}}/m_b)$ terms. With the calculation of these terms and the moments presented in this paper, global fits will allow precise determinations of $|V_{cb}|$ and m_b to occur from the inclusive decay spectrum.

As the precision of determinations of m_b and $|V_{cb}|$ improves, it becomes important to test the consistency of the OPE more precisely. Observables that do not depend strongly on the nonperturbative parameters that introduces the dominant uncertainty in extractions of m_b and $|V_{cb}|$ allow one to test if the uncertainty assigned for all higher order terms in the OPE is sufficiently large. By examining a general moment of the lepton spectrum [20], observables of this type, called OPE testing moments, have been found. In this paper, we apply this technique to hadronic invariant mass moments. By testing the error assigned to higher order effects experimentally we improve the confidence in the theoretical error assigned due to these effects in determinations of m_b and $|V_{cb}|$ from moments of semileptonic inclusive B decay. This allows extractions of m_b from inclusive semileptonic decay to occur in a theoretically clean and unambiguous fashion

*Electronic address: mrtrott@physics.utoronto.ca

[21]. These results can be combined with the results for the lepton energy spectrum for cross-checks and fits to determine the HQET parameters.

The structure of this paper is as follows. In Sec. II the $\mathcal{O}(\alpha_s)$ contribution to the hadronic tensor is presented. Section III reports on moments in the 1S mass scheme [22–25], and discusses the $m_b \Lambda_{\text{QCD}}/m_c$ expansion present in fractional hadronic invariant mass moments. The decay width to $\mathcal{O}(\alpha_s \Lambda_{\text{QCD}}/m_b)$ and $\mathcal{O}(\Lambda_{\text{QCD}}^3/m_b^3)$ and the error that should be assigned in the fit of the moments presented in this paper is discussed. The dominant parameters affecting the extraction of $|V_{cb}|$ inclusively, m_b^{1S} and λ_1 , are extracted from known moments. Observables appropriate to precisely test the consistency of the OPE are reported and moments that allow a measurement of the b quark mass with minimal theoretical error are presented.

II. $\mathcal{O}(\alpha_s)$ CONTRIBUTION TO DECAY SPECTRUM

A. Hadron tensor decomposition

The $\mathcal{O}(\alpha_s)$ corrections to semileptonic $B \rightarrow X_c \ell \bar{\nu}$ decay have been known for particular spectra and moments for some time [26–28]. The decomposition of the triple differential decay spectrum in terms of structure functions has not appeared in the literature to date, although the limit of this spectrum appropriate for a massless final state is known [29]. The triple differential decay spectrum must be known to allow for the experimentally required cuts on the kinematic variables to be imposed in calculating the $\mathcal{O}(\alpha_s \Lambda_{\text{QCD}}/m_b)$ terms and to perform a general moment analysis, and so we present it here.

We decompose the triple differential decay spectrum in terms of the invariant mass of the W boson $\hat{y} = q^2/m_b^2$ where q^μ is the momentum of the lepton pair, the c quark jet invariant mass $\hat{z} = (m_b v - q)^2/m_b^2$, and the charged lepton energy $\hat{E}_\ell = E_\ell/m_b$. This spectrum is written in terms of a lepton tensor $L_{\mu\nu}$ and the hadron tensor $W^{\mu\nu}$,

$$\frac{1}{\Gamma_0} \frac{d\Gamma}{d\hat{y} d\hat{z} d\hat{E}_\ell} = W^{\mu\nu}(\hat{y}, \hat{z}) L_{\mu\nu}(\hat{y}, \hat{z}, \hat{E}_\ell), \quad (1)$$

where

$$\Gamma_0 = \frac{G_F^2 |V_{cb}|^2 (m_b^{\text{pole}})^5}{192 \pi^3}. \quad (2)$$

Integrating over the charged lepton energy the differential decay spectrum becomes

$$\frac{1}{\Gamma_0} \frac{d\Gamma}{d\hat{y} d\hat{z}} = 12 E_0 t W_{\mu\nu}(\hat{y}, \hat{z}) L^{\mu\nu}(\hat{y}, \hat{z}), \quad (3)$$

where $E_0 = 1/2(1 + \hat{z} - \hat{y})$ is the leading order energy of

the c quark jet, $\rho = m_c^2/m_b^2$ and $t = \sqrt{1 - \hat{z}/E_0^2}$ is the rapidity of the c quark.

The hadron tensor can be decomposed in terms of the initial B meson four momentum Q^μ and the hadronic decay products four momentum $P^\mu = Q^\mu - q^\mu$, where q^μ is the momentum of the lepton pair. This tensor can be calculated from the discontinuity of the time ordered product of the current $J_\mu = \bar{c} \gamma_\mu (1 - \gamma_5) b$,

$$W^{\mu\nu} = \frac{1}{\pi \Gamma_0} \text{Im} \left[i \int d^4 x e^{i(P - m_b v) \cdot x} \langle \bar{B} | T [J^\dagger(x), J^\nu(0)] | \bar{B} \rangle \right]. \quad (4)$$

This tensor is calculated by considering the quark-gluon level processes involved in this decay. The spectra obtained from the parton level discontinuity are expected to accurately describe physical B meson decay spectra so long as observables are sufficiently inclusive.

The tensor decomposition in terms of the four vectors Q^μ and P^μ yields five nontrivial structure functions W_i ,

$$\begin{aligned} W^{\mu\nu}(\hat{y}, \hat{z}) = & W_1(\hat{y}, \hat{z})(P^\mu Q^\nu + P^\nu Q^\mu - P \cdot Q g^{\mu\nu} \\ & + i \epsilon^{\mu\nu\alpha\beta} Q_\alpha P_\beta) - W_2(\hat{y}, \hat{z}) g^{\mu\nu} \\ & + W_3(\hat{y}, \hat{z}) Q^\mu Q^\nu + W_4(\hat{y}, \hat{z})(P^\mu Q^\nu \\ & + P^\nu Q^\mu) + W_5(\hat{y}, \hat{z}) P^\mu P^\nu. \end{aligned} \quad (5)$$

The operator product expansion of the structure functions is known to $\mathcal{O}(\Lambda_{\text{QCD}}^3/m_b^3)$ [1–3,9]. There are two nonperturbative parameters at $\mathcal{O}(\Lambda_{\text{QCD}}^2/m_b^2)$ labeled $\lambda_{1,2}$ and six parameters at order $\mathcal{O}(\Lambda_{\text{QCD}}^3/m_b^3)$, labeled $\tau_{1,2,3,4}$ and $\rho_{1,2}$ the definitions of which can be found in [9].

B. $\mathcal{O}(\alpha_s)$ contributions to hadron tensor structure functions

The hadronic structure functions W_i in Eq. (5) have the perturbative expansion:

$$W_i(\hat{y}, \hat{z}) = W_i^0(\hat{y}, \hat{z}) + \frac{C_f \alpha_s}{4\pi} W_i^1(\hat{y}, \hat{z}) + \mathcal{O}(\alpha_s^2). \quad (6)$$

The $\mathcal{O}(\alpha_s)$ contributions to the structure functions are calculated by taking all cuts across all intermediate state contributions to the diagrams shown in Fig. 1. Combined with the external quark wave-function renormalization this gives the W_i^1 . At tree level, in the massless final state limit only W_1^0 is nonzero. W_1^1 can be expressed as

$$\begin{aligned} W_1^1(\hat{y}, \hat{z}) = & W_{1a}^1(E_0, t, \hat{z}, \hat{y}) \delta(\hat{z} - \rho) \\ & + W_{1b}^1(E_0, t, \hat{z}) \theta(\hat{z} - \rho) \\ & + W_{1c}^1(E_0, t, \hat{z}, \lambda_G^2), \end{aligned} \quad (7)$$

where

$$W_{1a}^1(E_0, t, \hat{z}, \hat{y}) = -16 - \frac{2}{t} \log^2\left(\frac{1+t}{1-t}\right) - \frac{4}{t} \log\left(\frac{1+t}{1-t}\right) \log(\rho) + \left(\frac{4(1+\rho)}{\hat{y}t} - \frac{12E_0}{\hat{y}t} + \frac{4\rho}{\hat{y}E_0t}\right) \log\left(\frac{1+t}{1-t}\right) \\ + \frac{(2-8E_0+6\rho)}{\hat{y}} \log(\rho) + \frac{8}{t} \text{Li}_2\left(\frac{2E_0t}{E_0(t-1)+1}\right) - \frac{8}{t} \text{Li}_2\left(\frac{2E_0t}{E_0(1+t)-\rho}\right) - \frac{8}{t} \left[\log\left(\frac{1+t}{1-t}\right) \right. \\ \left. + \log(\rho) \right] \log\left(\frac{1+(t-1)E_0}{\sqrt{\hat{y}}}\right),$$

$$W_{1b}^1(E_0, t, \hat{z}) = \frac{-2(1+\hat{z})(\hat{z}-\rho)}{\hat{z}E_0^2t^2} + \frac{2(5\hat{z}-\rho)}{\hat{z}E_0^2t^2} \\ - \frac{2(3\hat{z}+\rho)}{\hat{z}^2t^2} - \left(\frac{4}{E_0t^2} - \frac{(\hat{z}-\rho+4)}{E_0^2t^2}\right) \\ + \frac{(\hat{z}-\rho)}{E_0^3t^2} \frac{1}{t} \log\left(\frac{1+t}{1-t}\right),$$

$$W_{1c}^1(E_0, t, \hat{z}, \lambda_G^2) = -\left[16 - \frac{8}{t} \log\left(\frac{1+t}{1-t}\right)\right] \log(\lambda_G) \delta(\hat{z} \\ - \rho) - \theta[\hat{z} - (\sqrt{\rho} + \lambda_G)^2] \\ \times \frac{8\rho f_1}{\hat{z}(\hat{z}-\rho+\lambda_G^2)^2} - \theta[\hat{z} - (\sqrt{\rho} \\ + \lambda_G)^2] \frac{8f_1}{f_2} + \theta[\hat{z} - (\sqrt{\rho} + \lambda_G)^2] \\ \times \frac{8 \log\left(\frac{\hat{z}+\lambda_G^2-\rho+f_1t}{\hat{z}+\lambda_G^2-\rho-f_1t}\right)}{t(\hat{z}-\rho+\lambda_G^2)},$$

and

$$f_1 = \sqrt{\hat{z}^2 + (\lambda_G^2 - \rho)^2 - 2\hat{z}(\lambda_G^2 + \rho)}, \quad (8) \\ f_2 = \hat{z}^2 + 2E_0^2(1+t^2)\lambda_G^2 + (\lambda_G^2 - \rho)^2 - 2\hat{z}\rho.$$

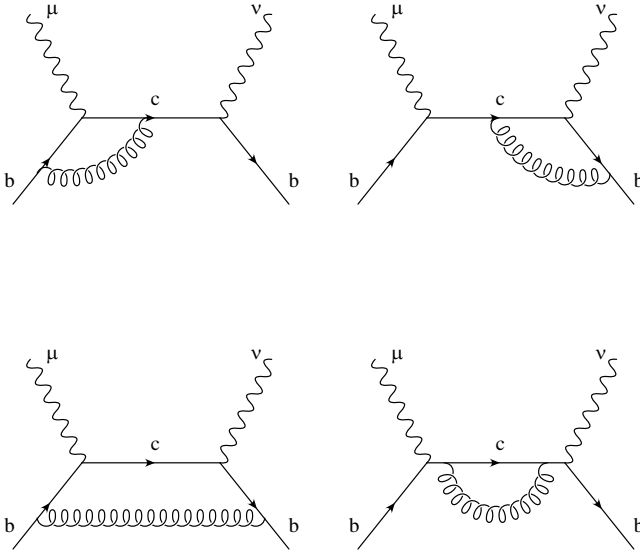


FIG. 1. The one loop forward scattering diagrams. The hadron tensor is derived by calculating the imaginary part of the diagrams.

The IR singularities present in the unintegrated spectra are regulated by a gluon mass λ_G in this calculation and the divergence cancels between the virtual and bremsstrahlung graphs once one integrates over phase space. The divergence directly cancels in integrations of these structure functions as the first two bremsstrahlung terms in W_{1c}^1 each contribute a factor of $8\log(\lambda_G)$, while the final term contributes a factor of $8/t\log[(1+t)/(1-t)]\log(\lambda_G)$. For the purposes of this paper it is sufficient to numerically integrate the $\mathcal{O}(\alpha_s)$ spectrum with the regulator assigned a small numerical value $\lambda_G \sim 10^{-6}$. The $\text{Li}_2(\hat{z})$ functions in W_{1c}^1 are the Dilogarithm functions, defined as $\text{Li}_2(\hat{z}) \equiv \sum_{k=1}^{\infty} (z^k/k^2)$ or equivalently, as $\text{Li}_2(\hat{z}) \equiv \int_z^0 [\log(1-t)/t] dt$. The other structure functions vanish at tree level in the limit $m_c \rightarrow 0$ and are IR safe at $\mathcal{O}(\alpha_s)$. For these structure functions we find

$$W_2^1(\hat{y}, \hat{z}) = W_{2a}^1(E_0, t, \hat{z}) \delta(\hat{z} - \rho) \\ + W_{2b}^1(E_0, t, \hat{z}) \theta(z - \rho), \quad (9)$$

$$W_{2a}^1(E_0, t, \hat{z}) = -\frac{2(\hat{z} + \rho)}{E_0t} \log\left(\frac{1+t}{1-t}\right),$$

$$W_{2b}^1(E_0, t, \hat{z}) = \frac{(\hat{z}^2 + 8\hat{z} - \rho^2)}{\hat{z}E_0t^4} - \frac{4(\hat{z} + \rho)}{E_0^2t^4} \\ - \frac{(\hat{z}^2 + 8\hat{z} - \rho^2)}{E_0^3t^4} + \frac{4\hat{z}(\hat{z} + \rho)}{E_0^4t^4} \\ + \left(-\frac{4}{E_0} + \frac{2(\hat{z} + \rho)}{E_0^2} - \frac{(\hat{z}^2 - 8\hat{z} - \rho^2)}{2E_0^3}\right) \\ - \frac{2\hat{z}(\hat{z} + \rho)}{E_0^4} + \frac{\hat{z}(\hat{z}^2 - \rho^2)}{2E_0^5} \frac{1}{t^5} \log\left(\frac{1+t}{1-t}\right),$$

$$W_3^1(\hat{y}, \hat{z}) = W_{3a}^1(E_0, t, \hat{y}) \delta(\hat{z} - \rho) \\ + W_{3b}^1(E_0, t, \hat{z}) \theta(z - \rho),$$

$$W_{3a}^1(E_0, t, \hat{y}) = \frac{\hat{z}}{\hat{y}} \left[\frac{-2(1+\hat{y}-\rho)}{E_0t} \right. \\ \left. \times \log\left(\frac{1+t}{1-t}\right) - 4\log(\rho) \right], \quad (10)$$

$$W_{3b}^1(E_0, t, \hat{z}) = \frac{16}{E_0 t^4} - \frac{14(\hat{z} - \rho)}{E_0^2 t^4} + \frac{3(\hat{z} - \rho)^2 - 16\hat{z}}{E_0^3 t^4} - 4\hat{z} \frac{(\hat{z} - \rho)}{E_0^4 t^4} + \left(-\frac{8}{E_0} + \frac{4(\hat{z} - \rho)}{E_0^2} - \frac{(\hat{z} - \rho)^2 - 8\hat{z}}{E_0^3} + \frac{5\hat{z}(\hat{z} - \rho)}{E_0^4} - \frac{\hat{z}(\hat{z} - \rho)^2}{2E_0^5} \right) \frac{1}{t^5} \log\left(\frac{1+t}{1-t}\right),$$

$$W_4^1(\hat{y}, \hat{z}) = W_{4b}^1(E_0, t, \hat{z})\theta(\hat{z} - \rho),$$

$$W_{4b}^1(E_0, t, \hat{z}) = \frac{2(\hat{z} - \rho)}{\hat{z}E_0 t^4} - \frac{(\hat{z} - \rho)^2}{\hat{z}E_0^2 t^4} + \frac{16(\hat{z} - \rho)}{E_0^3 t^4} - \frac{2(\hat{z} - \rho)^2}{E_0^4 t^4} + \left(\frac{-7(\hat{z} - \rho)}{E_0^3} + \frac{3(\hat{z} - \rho)^2}{2E_0^4} - \frac{2\hat{z}(\hat{z} - \rho)}{E_0^5} \right) \frac{1}{t^5} \log\left(\frac{1+t}{1-t}\right), \quad (11)$$

$$W_5^1(\hat{y}, \hat{z}) = W_{5a}^1(E_0, t, \hat{y})\delta(\hat{z} - \rho) + W_{5b}^1(E_0, t, \hat{z})\theta(\hat{z} - \rho),$$

$$W_{5a}^1(E_0, t, \hat{y}) = \frac{1}{\hat{y}} \left[\frac{2(1 - \hat{y} - \rho)}{E_0 t} \log\left(\frac{1+t}{1-t}\right) + 4 \log(\rho) \right],$$

$$W_{5b}^1(E_0, t, \hat{z}) = \frac{2(\hat{z}^2 - \rho^2)}{E_0 \hat{z}^2 t^4} - \frac{2(11\hat{z} - 3\rho)}{\hat{z}E_0^2 t^4} + \frac{(\hat{z} - \rho)^2 - 4\rho(\hat{z} - \rho)}{\hat{z}E_0^3 t^4} + \frac{4(\hat{z} + 3\rho)}{E_0^4 t^4} + \left(\frac{8}{E_0^2} - \frac{2(\hat{z} - \rho)}{E_0^3} + \frac{\hat{z} - 9\rho}{E_0^4} + \frac{\hat{z}^2 + 2\hat{z}\rho - 3\rho^2}{2E_0^5} \right) \frac{1}{t^5} \log\left(\frac{1+t}{1-t}\right). \quad (12)$$

We have checked the hadron tensor at $\mathcal{O}(\alpha_s)$ by integrating our results to compare against known $\mathcal{O}(\alpha_s)$ spectra and agree with [26] and the historical [30], but disagree, as do these other authors, with [27]. We also agree with the total $\mathcal{O}(\alpha_s)$ contribution to the decay rate in [31]. The massless limit of the $\mathcal{O}(\alpha_s)$ hadron structure functions has been taken for all regular terms and we find we agree with the regular terms for a massless final state [29].

C. Lepton tensor and phase space

To find moments of the triple differential spectrum one must integrate over phase space while imposing the experimentally required cut on the lepton energy. With no lepton energy cut the phase space is given by the follow-

ing region [26], referred to as region R_I :

$$\frac{1}{2}(b - \sqrt{b^2 - \hat{y}}) \leq \hat{E}_\ell \leq \frac{1}{2}(b + \sqrt{b^2 - \hat{y}}),$$

$$(\sqrt{\rho} + \lambda_G)^2 \leq \hat{z} \leq (1 - \sqrt{\hat{y}})^2, \quad (13)$$

$$0 \leq \hat{y} \leq (1 - \sqrt{\rho} - \lambda_G)^2,$$

where $b \equiv 1/2(1 - \hat{z} + \hat{y})$ and $\rho = m_c^2/m_b^2$. Without a lepton energy cut in the phase space, the lepton tensor integrated over the lepton energy \hat{E}_ℓ is

$$L_{\mu\nu}(\hat{y}, \hat{z}) = \hat{y}/3(-g_{\mu\nu} + \hat{q}_\mu \hat{q}_\nu / \hat{y}). \quad (14)$$

When a minimum cut $E_\ell^{\min} \geq xm_b$ is introduced, the phase space and the lepton tensor are modified. We do not repeat the derivation of the lepton tensor with a cut here, see [32], but note that the phase space splits into three regions when a cut is imposed. These three regions correspond to the partitioning of phase space that occurs when the electron energy lies below or within the phase space integration range as shown in Fig. 2. We only consider cuts below the upper limit of E_ℓ as given in Eq. (13), this corresponds to only considering cuts where $E_\ell^{\min} \leq m_b(1 - \sqrt{\rho})/2$.

For $x \leq 1/2(a - \sqrt{a^2 - \hat{y}})$, where $a \equiv 1/2[1 - (\sqrt{\rho} + \lambda_G)^2 + \hat{y}]$ the cut, labeled as x_1 in Fig. 2, is below the lower limit of the lepton energy in Eq. (13) and as the integration over the lepton energy is unaffected, the lepton tensor with this cut reduces to the simple expression above with the electron energy integrated over

$$\frac{1}{2}(b - \sqrt{b^2 - \hat{y}}) \leq \hat{E}_\ell \leq \frac{1}{2}(b + \sqrt{b^2 - \hat{y}}). \quad (15)$$

However, this lepton energy cut still affects the subsequent integrations of \hat{z} and \hat{y} by imposing the constraint on the range of \hat{y} ,

$$[1 - (\sqrt{\rho} + \lambda_G)^2 - 2x] \frac{2x}{1 - 2x} \leq \hat{y}, \quad (16)$$

so that the remaining kinematic variables are integrated over the phase space region R_{II} ,

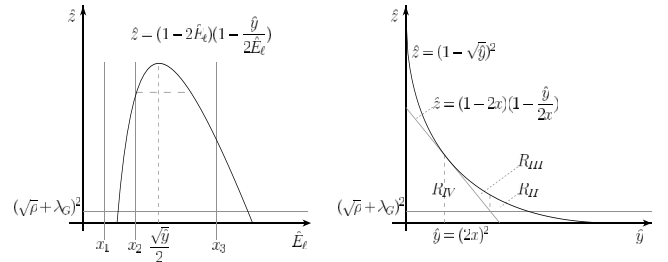


FIG. 2. Phase space diagrams with a lepton energy cut.

$$(\sqrt{\rho} + \lambda_G)^2 \leq \hat{z} \leq (1 - \sqrt{\hat{y}})^2, \quad (17)$$

$$[1 - (\sqrt{\rho} + \lambda_G)^2 - 2x] \frac{2x}{1 - 2x} \leq \hat{y} \leq (1 - \sqrt{\rho} - \lambda_G)^2.$$

For $x \geq 1/2(a - \sqrt{a^2 - \hat{y}})$ while $x \leq \sqrt{\hat{y}}/2$, labeled in the diagram as the cut x_2 , the phase space splits into two regions. The first region R_{III} has the hadron tensor contracted with the lepton tensor of Eq. (14), and the range of \hat{E}_ℓ as given by Eq. (15). The remaining phase space variables are then integrated over the range,

$$(1 - 2x) \left(1 - \frac{\hat{y}}{2x}\right) \leq \hat{z} \leq (1 - \sqrt{\hat{y}})^2, \quad (18)$$

$$(2x)^2 \leq \hat{y} \leq [1 - (\sqrt{\rho} + \lambda_G)^2 - 2x] \frac{2x}{1 - 2x}.$$

The second region of type R_{III} combines with the region of phase space where $x \geq 1/2(a - \sqrt{a^2 - \hat{y}})$ while $x \geq \sqrt{\hat{y}}/2$, labeled as x_3 on Fig. 2. The resulting combined phase space has the lepton tensor incorporating the cut within the phase space range and the subsequent integration is given by the region R_{IV} ,

$$x \leq \hat{E}_\ell \leq \frac{1}{2}(b + \sqrt{b^2 - \hat{y}}),$$

$$(\sqrt{\rho} + \lambda_G)^2 \leq \hat{z} \leq (1 - 2x) \left(1 - \frac{\hat{y}}{2x}\right), \quad (19)$$

$$0 \leq \hat{y} \leq [1 - (\sqrt{\rho} + \lambda_G)^2 - 2x] \frac{2x}{1 - 2x}.$$

III. HADRONIC MASS MOMENTS

A. 1S mass scheme

In calculating moments of the hadronic invariant mass spectrum, we use the 1S mass and the epsilon expansion [22,23]. It is well known the pole mass renormalon [24,25] ambiguity leads to unnecessarily badly behaved perturbation series for moments when a poor mass scheme is chosen. In the 1S scheme the renormalon ambiguity is of $\mathcal{O}(\Lambda_{\text{QCD}}^4/m_b^4)$ and so we expect the perturbation series of moments of the spectra to be better behaved. We express moments in terms of the 1S mass, which is related to the b quark pole mass through the relation [22,23]

$$\frac{m_b^{\text{1S}}}{m_b^{\text{pole}}} = 1 - \frac{(\alpha_s C_F)^2}{8} \left\{ 1\epsilon + \frac{\alpha_s}{\pi} \left[\left(\ell + \frac{11}{6} \right) \beta_0 - 4 \right] \times \epsilon^2 + \mathcal{O}(\epsilon^3) \right\}, \quad (20)$$

where $\ell = \log[\mu/(m_b \alpha_s C_F)]$ and $C_F = 4/3$. The parameter $\epsilon = 1$ determines the order in the modified perturbative expansion. Using the epsilon expansion

necessitates introducing a modified perturbative expansion in order to ensure the cancellation of renormalon ambiguities [22]. When calculating in the 1S mass scheme the $\mathcal{O}(\alpha_s^n)$ perturbative corrections coming from the mass transformation Eq. (20) are counted using the parameter ϵ^{n-1} , while $\mathcal{O}(\alpha_s^n)$ corrections in the decay rate are counted as ϵ^n .

The dependence on the pole mass of the charm quark in our results is eliminated through

$$\begin{aligned} m_b^{\text{pole}} - m_c^{\text{pole}} &= \bar{m}_B - \bar{m}_D + \lambda_1 \left(\frac{2\bar{m}_D - m_Y}{2m_Y \bar{m}_D} \right) \\ &+ \lambda_1 \frac{m_Y - 2\bar{m}_B}{4\bar{m}_D^2} + \lambda_1 \Lambda_{\text{1S}} \frac{4\bar{m}_D^2 - m_Y^2}{2\bar{m}_D^2 m_Y^2} \\ &- (\tau_1 + \tau_3 - \rho_1) \frac{m_Y^2 - 4\bar{m}_D^2}{4\bar{m}_D^2 m_Y^2} \\ &+ \mathcal{O}(\Lambda_{\text{QCD}}^4/m_b m_c^2). \end{aligned} \quad (21)$$

The meson masses \bar{m}_D and \bar{m}_B are the spin averaged meson masses $\bar{m}_X = (m_X + 3m_{X^*})/4$. In this relation we use the fact that $\frac{m_Y}{2} - m_b^{\text{1S}} \sim \Lambda_{\text{QCD}}$ and expand in the parameter Λ_{1S}

$$\Lambda_{\text{1S}} \equiv \frac{m_Y}{2} - m_b^{\text{1S}}. \quad (22)$$

The perturbative corrections coming from expressing the b quark mass in terms of the 1S mass are determined by using the definitions of Λ_{1S} and m_b^{1S} and the HQET relationship between meson masses and quark masses

$$\begin{aligned} m_H &= m_Q + \bar{\Lambda} - \frac{\lambda_1 + d_H \lambda_2}{2m_Q} + \frac{\rho_1 + d_H \rho_2}{4m_Q^2} \\ &- \frac{\tau_1 + \tau_3 + d_H(\tau_2 + \tau_4)}{4m_Q^2} + \mathcal{O}\left(\frac{\Lambda_{\text{QCD}}^4}{m_Q^3}\right), \end{aligned} \quad (23)$$

where m_H is the hadronic mass, m_Q is the heavy quark mass, and $d_H = 3$ for the pseudoscalar mesons while $d_H = -1$ for the vector mesons.

In calculating the general hadronic moment, previously calculated moments by Bauer, Ligeti, Luke and Manohar (BLLM) [17] were reexamined in the 1S mass scheme to check results. The results presented in the following sections for the first hadronic moment and its variance are different for two reasons. First, in BLLM a $1/\bar{m}_B$ expansion was used to replace m_B in the expansion of s_H in terms of partonic variables,

$$\begin{aligned} m_B &= \bar{m}_B + \frac{3(m_Y - 4\bar{m}_B)\lambda_2}{4\bar{m}_B^2} - \frac{3\lambda_2 \Lambda_{\text{1S}}}{2\bar{m}_B^2} \\ &- \frac{3}{4\bar{m}_B^2}(\tau_2 + \tau_4) + \frac{3}{4\bar{m}_B^2}\rho_2 + \mathcal{O}\left(\epsilon, \frac{\Lambda_{\text{QCD}}^4}{m_B^3}\right). \end{aligned} \quad (24)$$

In the results reported in the following sections we always use a $1/m_Y$ expansion. The corresponding expansion is

$$m_B = \bar{m}_B - \frac{3\lambda_2}{m_Y} - \frac{6\lambda_2\Lambda_{1S}}{m_Y^2} - \frac{3}{m_Y^2}(\tau_2 + \tau_4) + \frac{3}{m_Y^2}\rho_2 + \mathcal{O}\left(\epsilon, \frac{\Lambda_{\text{QCD}}^4}{m_Y^3}\right). \quad (25)$$

Second, we treat a class of powers of $(\bar{m}_B - m_Y/2)^n$ differently than BLLM. When terms are generated by changing $\bar{\Lambda} \equiv m_B - m_b$ into Λ_{1S} ,

$$\bar{\Lambda} = \left(\bar{m}_B - \frac{m_Y}{2}\right) + \Lambda_{1S} + \frac{\lambda_1}{m_Y} + \frac{2\Lambda_{1S}\lambda_1}{m_Y^2} + \frac{(\tau_1 + \tau_3 - \rho_1)}{m_Y^2} + \mathcal{O}\left(\epsilon, \frac{\Lambda_{\text{QCD}}^4}{m_Y^3}\right), \quad (26)$$

the $(\bar{m}_B - m_Y/2)^n$ terms are kept only for $n \leq 3$. In BLLM this class of terms are treated as $\mathcal{O}(1)$ although they are formally of order Λ_{QCD}^n , leading to this class of higher order terms of $(\bar{m}_B - m_Y/2)^n$ being kept and summed into the coefficients of the nonperturbative pa-

rameters. In the following results, the $(\bar{m}_B - m_Y/2)^n$ terms from $\bar{\Lambda}$ are counted as order Λ_{QCD}^n and in the results of Sec. III they are kept only up to $\mathcal{O}(\Lambda_{\text{QCD}}^3)$ in the non-perturbative expansion and up to $\mathcal{O}(\Lambda_{\text{QCD}})$ for perturbative terms. Factors of $(\bar{m}_B - m_Y/2)$ are also generated in the replacement of the c and b quark mass and these factors are treated as $\mathcal{O}(1)$. This implementation of the 1S scheme is similar to the general moment analysis of the lepton energy spectrum [20]. The lepton moments are presented in Appendix C and can be combined with the hadronic spectrum results to cross-check extractions of Λ_{1S} and λ_1 from these differing spectra. Further hadronic moments that are appropriate for a global fit, such as $s_H^{1/2}$ and $s_H^{3/2}$ are presented in Appendix B.

B. Decay width to $\mathcal{O}(\alpha_s\Lambda_{\text{QCD}}/m_b)$, $\mathcal{O}(\Lambda_{\text{QCD}}^3/m_b^3)$

With the 1S scheme implemented as discussed in the previous section, the decay width of $B \rightarrow X_c \ell \bar{\nu}$ is

$$\Gamma(B \rightarrow X_c \ell \bar{\nu}) = \Gamma_0 \left[0.5325 - 1.132 \frac{\Lambda_{1S}}{m_Y/2} - 0.924 \left(\frac{\Lambda_{1S}}{m_Y/2}\right)^2 - 1.89 \left(\frac{\Lambda_{1S}}{m_Y/2}\right)^3 - 2.12 \frac{\lambda_1}{(m_Y/2)^2} - 3.93 \frac{\lambda_2}{(m_Y/2)^2} + 0.74 \frac{\lambda_1 \Lambda_{1S}}{(m_Y/2)^3} - 1.73 \frac{\lambda_2 \Lambda_{1S}}{(m_Y/2)^3} - 5.99 \frac{\rho_1}{(m_Y/2)^3} + 4.94 \frac{\rho_2}{(m_Y/2)^3} - 2.98 \frac{\tau_1}{(m_Y/2)^3} + 0.99 \frac{\tau_2}{(m_Y/2)^3} - 4.96 \frac{\tau_3}{(m_Y/2)^3} - 4.94 \frac{\tau_4}{(m_Y/2)^3} - 0.080\epsilon + 0.133\epsilon \frac{\Lambda_{1S}}{m_Y/2} + 0.004\epsilon \left(\frac{\Lambda_{1S}}{m_Y/2}\right)^2 \right], \quad (27)$$

where $\Gamma_0 = (G_F^2 |V_{cb}|^2 / 192\pi^3) (m_Y/2)^5$. Uncertainties in the values of Λ_{1S} , λ_i , ρ_i and τ_i introduce uncertainties in the inclusive extractions of $|V_{cb}|$ using the decay width. In the nonperturbative expansion the largest theoretical uncertainty in the extraction of $|V_{cb}|$ comes from Λ_{1S} and λ_1 which one can see introduce $\sim 2\%$ uncertainties, followed by the higher order nonperturbative terms which impose an uncertainty of $\sim 1\%$ as one can see by examining the results for the total decay width and estimating the size of the unknown terms with dimensional analysis.

The size of the $\mathcal{O}(\alpha_s^2)$ can be estimated by calculating the $\alpha_s^2 \beta_0$ contribution to $\mathcal{O}(\alpha_s^2)$ [17,33,34], although these terms are not included in this paper. This has been done in the 1S scheme for a number of observables and the full size of these corrections being treated as an error introduces $\sim 2\%$ uncertainty in the extraction of $|V_{cb}|$. The next largest uncalculated contributions in the decay width are the $\mathcal{O}(\alpha_s \lambda_i)$ and $\mathcal{O}(\alpha_s \Lambda_{1S})$ terms and the $\mathcal{O}(\Lambda_{\text{QCD}}^4/m_b^2 m_c^2)$ neglected terms. The size of the $\mathcal{O}(\alpha_s \Lambda_{\text{QCD}}^2/m_b^2)$ terms in the 1S scheme may be estimated by taking the size of the $\alpha_s \Lambda_{1S}$ and multiplying by $\Lambda_{\text{QCD}}/m_b \sim 0.1$. For the first moment, this indicates that the order of the $\alpha_s \lambda_i$ terms is expected to be $\sim 0.01 \Lambda_{\text{QCD}}^2$ which can be safely neglected in fits to determine the third order parameters in the OPE. However, completely

uncorrelated uncertainties of this size for both $\alpha_s \lambda_i$ should be used to estimate the error on the fit. The size of the corrections introduced when using the mass splitting formula to replace the c quark mass should also be estimated in a fit to extract the third order terms in the OPE, as well as uncertainties due to $1/m_b^4$ corrections to the OPE. The number and size of these terms are completely unknown and the uncertainties introduced due to these terms can be estimated by introducing completely uncorrelated errors of their naive dimensional size.

C. Integral hadronic moments

The nonperturbative parameters in the decay width can be determined by global fits to moments calculated from the decay spectra of $B \rightarrow X_c \ell \bar{\nu}$ such as the hadronic invariant mass spectra. The first and second moments of the hadronic invariant mass spectrum have been known for some time [8,28]. The perturbative corrections to these moments were obtained by expressing the hadronic moments in terms of the known $\mathcal{O}(\alpha_s)$ corrections to the lepton spectra and the leading order hadronic invariant mass spectra. This technique fails when a lepton energy cut is introduced into the phase space, and the general tensor results of Sec. II are required. In terms of partonic

TABLE I. Coefficients of the nonperturbative parameters for $S_1(E_0)$.

E_ℓ^{\min}	S_1^0	Λ_{1S}	Λ_{1S}^2	Λ_{1S}^3	λ_1	λ_2	$\lambda_1\Lambda_{1S}$	$\lambda_2\Lambda_{1S}$	ρ_1	ρ_2	τ_1	τ_2	τ_3	τ_4
0	0.834	1.646	0.451	0.16	1.43	-0.34	0.51	0.07	0.71	-0.34	0.32	0.25	0.29	0.15
0.5	0.822	1.623	0.445	0.16	1.44	-0.30	0.51	0.09	0.72	-0.34	0.32	0.26	0.29	0.16
0.7	0.807	1.592	0.435	0.16	1.46	-0.24	0.53	0.12	0.75	-0.34	0.33	0.27	0.29	0.17
0.9	0.786	1.549	0.420	0.16	1.51	-0.14	0.55	0.18	0.79	-0.34	0.34	0.30	0.30	0.18
1.1	0.762	1.496	0.397	0.15	1.57	0.00	0.59	0.26	0.87	-0.33	0.35	0.34	0.31	0.21
1.3	0.737	1.439	0.368	0.15	1.69	0.18	0.66	0.37	0.99	-0.30	0.37	0.41	0.32	0.24
1.5	0.719	1.392	0.334	0.14	1.92	0.42	0.79	0.51	1.23	-0.23	0.41	0.53	0.33	0.28

quantities the hadronic invariant mass is defined to be

$$s_H = (Q - q)^2 = m_B^2 - m_B m_b (1 - \hat{z} + \hat{y}) + m_b^2 \hat{y}. \quad (28)$$

It is conventional to examine the first hadronic moment once the spin averaged meson mass \bar{m}_D^2 is subtracted. Moments that give the mean and variance of the hadronic invariant mass spectrum with lepton energy cuts of differing values were reexamined recently by BLLM. These moments are defined with lepton energy cuts E_ℓ^{\min} ,

$$\begin{aligned} S_1(E_\ell^{\min}) &= \langle s_H - \bar{m}_D^2 \rangle |_{E_i \geq E_\ell^{\min}}, \\ S_2(E_\ell^{\min}) &= \langle (s_H - \langle s_H \rangle)^2 \rangle |_{E_i \geq E_\ell^{\min}}. \end{aligned} \quad (29)$$

These moments as functions of the cut on the lepton energy, including the previously uncalculated perturbative corrections are as follows. The coefficients stated are for the dimensional nonperturbative parameters listed at the top of the column. The data used in the numerical evaluations in this paper are $\bar{m}_B = 5.3135$ GeV, $\bar{m}_D = 1.9730$ GeV, $m_\gamma = 9.4603$ GeV and the strong coupling is $\alpha_s(m_b) = 0.22$. For example for the first moment with no cut we find

$$\begin{aligned} S_1(0) &= 0.834 + 1.646\Lambda_{1S} + 0.451\Lambda_{1S}^2 + 0.16\Lambda_{1S}^3 \\ &+ 1.43\lambda_1 - 0.34\lambda_2 + 0.51\lambda_1\Lambda_{1S} + 0.07\lambda_2\Lambda_{1S} \\ &+ 0.71\rho_1 - 0.34\rho_2 + 0.32\tau_1 + 0.25\tau_2 + 0.29\tau_3 \\ &+ 0.15\tau_4 + 0.143\epsilon + 0.175\Lambda_{1S}\epsilon, \end{aligned} \quad (30)$$

and in the following Tables I and II the leading order term of a moment S_i is labeled S_i^0 .

For the $S_2(E_0)$ moments, as explained in Sec. III A, the results differ from those stated in BLLM. This difference is formally of higher order, and in the nonperturbative expansion the overall effect of the differing implementations of the 1S scheme is small. The effect of these terms in the perturbative expansion is also small for most moments. However, the variance of the hadronic invariant mass spectrum is more sensitive to higher order terms due to the cancellation among leading order terms in the nonperturbative expansion. The 1S scheme as implemented in BLLM found that the variance increased as the lepton energy cut was increased due to the dominance of the $\mathcal{O}(\alpha_s)$ term and the suppression of leading order nonperturbative corrections. The $\mathcal{O}(\alpha_s)$ term is the dominant correction to the variance in the $m_b \rightarrow \infty$ limit. The experimentally measured lepton energy cut dependence has the variance decreasing as the lepton energy cut increases. When $(\bar{m}_B - m_\gamma/2)$ terms are treated as detailed in Sec. III A in the 1S scheme, the $\mathcal{O}(\alpha_s)$ term and variance has the experimentally measured dependence on the lepton energy cut, as can be seen in Tables III and IV.

The moments S_1 and S_2 with a lepton energy cut of 1.5 GeV have been experimentally measured by CLEO [12],

$$S_1(1.5 \text{ GeV}) = 0.251 \pm 0.066 \text{ GeV}^2, \quad (31)$$

$$S_2(1.5 \text{ GeV}) = 0.576 \pm 0.170 \text{ GeV}^4. \quad (32)$$

Using this data, we can extract values of Λ_{1S} and λ_1 , for comparison with extractions from the lepton energy spectrum. We estimate the theoretical error on the extrac-

TABLE II. Coefficients of the perturbative parameters for $S_1(E_0)$.

E_ℓ^{\min}	1S α_s^2 Contribution		α_s Contribution		Combined $\mathcal{O}(\epsilon)$	
	ϵ	$\Lambda_{1S} \epsilon$	ϵ	$\Lambda_{1S} \epsilon$	ϵ	$\Lambda_{1S} \epsilon$
0	-0.014	0.090	0.157	0.086	0.143	0.175
0.5	-0.014	0.088	0.143	0.069	0.129	0.157
0.7	-0.014	0.086	0.139	0.072	0.125	0.159
0.9	-0.014	0.084	0.134	0.076	0.120	0.160
1.1	-0.014	0.081	0.128	0.080	0.114	0.161
1.3	-0.015	0.077	0.121	0.085	0.106	0.162
1.5	-0.018	0.073	0.117	0.093	0.099	0.166

TABLE III. Coefficients of the nonperturbative parameters for $S_2(E_0)$.

E_ℓ^{\min}	S_2^0	Λ_{1S}	Λ_{1S}^2	Λ_{1S}^3	λ_1	λ_2	$\lambda_1\Lambda_{1S}$	$\lambda_2\Lambda_{1S}$	ρ_1	ρ_2	τ_1	τ_2	τ_3	τ_4
0	0.0163	0.09	0.08	-0.03	-4.87	1.33	-1.85	2.04	-6.41	1.51	-1.04	-2.87	0.00	0.25
0.5	0.0152	0.08	0.07	-0.03	-4.78	1.34	-1.79	2.07	-6.48	1.39	-1.03	-2.82	0.00	0.25
0.7	0.0153	0.08	0.07	-0.03	-4.65	1.35	-1.70	2.09	-6.61	1.23	-1.01	-2.77	0.00	0.25
0.9	0.0167	0.09	0.07	-0.04	-4.48	1.37	-1.56	2.12	-6.84	0.99	-0.98	-2.69	0.00	0.25
1.1	0.0195	0.10	0.08	-0.04	-4.26	1.40	-1.36	2.17	-7.23	0.68	-0.95	-2.61	0.00	0.24
1.3	0.0224	0.11	0.09	-0.04	-4.01	1.44	-1.10	2.25	-7.88	0.28	-0.92	-2.53	0.00	0.24
1.5	0.0227	0.11	0.09	-0.04	-3.76	1.52	-0.77	2.38	-9.05	-0.22	-0.91	-2.48	0.00	0.24

tion due to the unknown third order terms in the usual way [9] using the results of recent fits when they substantially improve our knowledge of these terms beyond dimensional analysis. We use the HQET vector pseudo-scalar mass splitting constraint to determine $\lambda_2 = 0.12 \text{ GeV}^2$ and the mass splitting formula to third order [8],

$$\rho_2 - \tau_2 - \tau_4 = \frac{\kappa(m_c)m_b^2 m_c \Delta m_B - m_b m_c^2 \Delta m_D}{m_b - m_c \kappa(m_c)}, \quad (33)$$

to reduce the number of free parameters. A positive value of ρ_1 is imposed in accordance with vacuum saturation [35] and is drawn from the range $[0, 0.125] \text{ GeV}^3$. The unknown matrix elements are then drawn from a flat distribution, the unknown third order terms are drawn from between $\pm 0.125 \text{ GeV}^3$ while λ_1 is drawn from $[-600, 0] \text{ MeV}^2$ in accordance with its full constrained range from the BLLM fit. We then extract the following values for λ_1 and Λ_{1S} :

$$\begin{aligned} \Lambda_{1S} &= [-0.13 \pm 0.05_\epsilon \pm 0.09_{m^3}] \text{ GeV}, \\ \lambda_1 &= [-0.24 \pm 0.02_\epsilon \pm 0.09_{m^3}] \text{ GeV}^2. \end{aligned} \quad (34)$$

The perturbative errors are estimated by using the two loop running of α_s to vary the scale of $\alpha_s(\mu)$ between $m_b/2 < \mu < 2m_b$. Adding the theoretical errors in quadrature we obtain $m_b^{\text{IS}} = 4.86 \pm 0.10 \text{ GeV}$, which is in excellent agreement with the inclusive extraction using the lepton energy moments, $m_b^{\text{IS}} = 4.84 \pm 0.10 \text{ GeV}$ [20] and in agreement with the results of BLLM where $m_b^{\text{IS}} = 4.74 \pm 0.10 \text{ GeV}$, despite the differences in the expansion

and the larger number of observables in the fit. This extracted 1S mass $m_b^{\text{IS}} = 4.86 \pm 0.10 \text{ GeV}$ translates into a value of the $\overline{\text{MS}}$ mass $\bar{m}_b(m_b) = 4.34 \pm 0.09 \text{ GeV}$ which can be compared with other extractions of the $\overline{\text{MS}}$ mass [21] such as the $\overline{\text{MS}}$ mass found by examining moments of the $b\bar{b}$ production cross section [36–40] a recent analysis of which finds $\bar{m}_b(m_b) = 4.25 \pm 0.08 \text{ GeV}$ [41].

D. Fractional moments

1. The $1/m_c$ expansion

In integer moments such as S_1 and S_2 , a Λ_{QCD}/m_c expansion only enters the predicted value of a moment through the mass transformation relationship Eq. (21). Fractional moments have additional cuts in the complex $q \cdot v$ plane due to the branch cut starting at $s_H = 0$ when s_H is taken to a noninteger power. These branch cuts are separated from the physical cut by a scale set by m_c , as the physical branch cut begins at $s_H = m_D^2$. As $m_c \rightarrow 0$ these cuts coalesce and one would expect predictions for fractional moments in this limit to be ill defined, as discussed in recent work [19]. We find an explicit $m_b \Lambda_{\text{QCD}}/m_c^2$ expansion in calculations of fractional moments of s_H ; the neglected terms in this expansion are numerically suppressed for hadronic invariant mass observables leading to a small numerical uncertainty being introduced. This can be shown by examining a general moment of the squared hadronic invariant mass s_H^n . The dependence of the general moment as a function of n is found by performing a binomial expansion of s_H^n ,

TABLE IV. Coefficients of the perturbative parameters for $S_2(E_0)$.

E_ℓ^{\min}	1S α_s^2 Contribution		α_s Contribution		Combined $O(\epsilon)$	
	ϵ	$\Lambda_{1S} \epsilon$	ϵ	$\Lambda_{1S} \epsilon$	ϵ	$\Lambda_{1S} \epsilon$
0	0.105	0.163	0.551	0.424	0.656	0.588
0.5	0.102	0.159	0.163	-0.202	0.265	-0.043
0.7	0.099	0.154	0.099	-0.266	0.198	-0.112
0.9	0.094	0.147	0.057	-0.283	0.151	-0.136
1.1	0.089	0.140	0.029	-0.273	0.118	-0.132
1.3	0.085	0.135	0.010	-0.240	0.096	-0.112
1.5	0.083	0.133	0.002	-0.211	0.083	-0.078

TABLE V. Coefficients of the nonperturbative parameters for OPE testing moments. The OPE testing moments in the table are defined in the following way: $D_a^1 = S[2.0, 0.5, 2.2, 0.7]$, $D_b^2 = S[1.9, 0.6, 2, 0.7]$, $D_c^3 = S[2.6, 0.6, 2.9, 1]$, $D_d^4 = S[2.4, 1, 1.9, 0.8]$ and $D_e^5 = S[2.9, 1.4, 2.2, 1.3]$.

	Λ_{1S}	Λ_{1S}^2	Λ_{1S}^3	λ_1	λ_2	$\lambda_1\Lambda_{1S}$	$\lambda_2\Lambda_{1S}$	ρ_1	ρ_2	τ_1	τ_2	τ_3	τ_4	
D_a^1	0.7779	-0.028	0.01	0.00	0.00	-0.04	-0.01	-0.06	0.05	-0.00	0.00	0.03	-0.01	-0.01
D_b^2	0.8845	-0.019	0.00	0.00	0.00	-0.02	-0.01	-0.03	0.03	0.00	0.00	0.01	-0.01	-0.01
D_c^3	0.7829	0.047	0.10	0.04	0.00	-0.13	-0.03	-0.16	0.06	0.03	0.00	0.03	-0.02	-0.02
D_d^4	1.9030	0.166	-0.08	-0.03	0.00	0.22	0.08	0.38	-0.27	0.00	-0.01	-0.15	0.06	0.07
D_e^5	2.428	0.040	-0.46	-0.20	0.00	0.66	0.19	0.99	-0.62	-0.08	-0.03	-0.29	0.12	0.14

$$s_H^n = \sum_{k=0}^{\infty} \sum_{l=0}^k \frac{\Gamma(n+1)}{\Gamma(n+1-k)\Gamma(k)} C_l^k \hat{y}^l \hat{z}^{n-k} m_b^{2n}. \quad (35)$$

The coefficient functions C_l^k are $O(\Lambda_{\text{QCD}}^k/m_b^k)$. Expanding up to $O(\Lambda_{\text{QCD}}^3/m_b^3)$ in the nonperturbative expansion we find

$$s_H^n = \hat{z}^n m_b^{(2n)} \left[C_0^0 + \frac{n}{\hat{z}} (C_0^1 + \hat{y} C_1^1) + \frac{n(n-1)}{1!\hat{z}^2} \times (C_0^2 + \hat{y} C_1^2 + \hat{y}^2 C_2^2) + \frac{n(n-1)(n-2)}{2!\hat{z}^3} \times (C_0^3 + \hat{y} C_1^3 + \hat{y}^2 C_2^3 + \hat{y}^3 C_3^3) \right], \quad (36)$$

where the C_l^k are functions of n and the nonperturbative matrix elements.¹ For integer moments this expression has no $1/z$ dependence. However, for noninteger moments in this range one obtains contributions of order z^{-k} where $k \geq n$ is the ceiling of the fractional moment power n . As the lower limit of z is $\rho = m_c^2/m_b^2$, this corresponds to a $m_b \Lambda_{\text{QCD}}/m_c$ expansion entering into the calculations of fractional moments. This expansion does not seem to introduce a large uncertainty for fractional moments compared to integer moments as the neglected class of terms is numerically suppressed for n values in the range $[0, 3]$ but the best way to estimate the uncertainty introduced is under study. In the following investigation of hadronic fractional moments no additional uncertainty is added to account for this theoretical error and we examine how known sources of error primarily from unknown matrix elements can be reduced.

When examining a general moment s_H^n to obtain interesting observables, we expand in the ratio Λ_{QCD}/m_Q and then examine the n and E_ℓ^{min} dependence of the coefficient functions of the nonperturbative matrix elements. The essential observation motivating this approach is that one is allowed to choose n and E_ℓ^{min} within a range of reasonably accessible experimental values, in order to maximize the utility of a measured moment in obtaining information on the nonperturbative matrix elements. We define a general moment function,

¹These C_l^k coefficient functions are reported in Appendix A.

$$S[n, E_{\ell_1}, m, E_{\ell_2}] = \frac{\langle s_H^n \rangle |_{E_i \geq E_1}}{\langle s_H^m \rangle |_{E_i \geq E_2}}, \quad (37)$$

so that

$$S_1(E_\ell^{\text{min}}) = S[1, E_\ell^{\text{min}}, 0, E_\ell^{\text{min}}] - \bar{m}_D^2, \\ S_2(E_\ell^{\text{min}}) = S[2, E_\ell^{\text{min}}, 0, E_\ell^{\text{min}}] - (S[1, E_\ell^{\text{min}}, 0, E_\ell^{\text{min}}])^2.$$

Our search of the hadronic mass moments is restricted to the parameter space,

$$m < 3, \quad n < 3, \quad 0.5 \text{ GeV} < E_{\ell_i}^{\text{cut}} < 1.5 \text{ GeV}, \quad (38)$$

to ensure a well-behaved OPE. In this parameter space we find two types of moments of interest, moments that allow the OPE to be precisely tested for deviations from experiment and moments that allow one to extract the 1S mass with minimal error. We consider each type of moment in the following sections.

2. OPE testing moments

A discrepancy of the prediction of the OPE when compared with data can come from a number of possible sources when one is considering percent level extractions of $|V_{cb}|$: a higher order matrix element that is being neglected could be anomalously large, the OPE itself could not be converging or quark-hadron duality violation could effect determinations [42–47]. By finding moments where only the leading order unknown nonperturbative parameters are suppressed and checking the predicted values against experiment, one can assess the theoretical error that is being assigned to the inclusive extraction of $|V_{cb}|$ in a clear and unambiguous fashion. This technique [20] has recently been used to test the OPE in the lepton energy spectrum. Measurements of these OPE testing observables in this spectrum indicated that the OPE is a valid description of the data to the percent level [48]. It is important to note that the OPE testing moments presented allow one to check that the error assigned in the extractions of $|V_{cb}|$ and m_b is large enough to account for all of these possible effects

TABLE VI. Coefficients of the perturbative parameters for OPE testing moments and their predicted value.

Label	1S α_s^2 Term		α_s Term		Combined $O(\epsilon)$		Predicted value for moment
	ϵ	$\Lambda_{1S} \epsilon$	ϵ	$\Lambda_{1S} \epsilon$	ϵ	$\Lambda_{1S} \epsilon$	
D_a^1	-0.001	-0.005	-0.006	-0.001	-0.007	-0.007	$0.7686 \pm 0.0018\epsilon \pm 0.0040(\text{N.P.})$
D_b^2	-0.001	-0.003	-0.005	-0.004	-0.006	-0.007	$0.8804 \pm 0.0014\epsilon \pm 0.0025(\text{N.P.})$
D_c^3	-0.001	-0.004	-0.005	-0.012	-0.006	-0.016	$0.7582 \pm 0.0016\epsilon \pm 0.0067(\text{N.P.})$
D_d^4	0.006	0.029	0.025	-0.012	0.030	0.017	$1.9448 \pm 0.0078\epsilon \pm 0.026(\text{N.P.})$
D_e^5	0.010	0.050	0.026	-0.036	0.036	0.014	$2.5380 \pm 0.0102\epsilon \pm 0.047(\text{N.P.})$

if the OPE testing moments properly describe the data [49]. (A selection of these OPE testing moments for the hadronic invariant mass spectrum is presented in Table V.) The nonperturbative parameters for these moments are not suppressed except for the leading unknown nonperturbative terms Λ_{1S} and λ_1 . A typical OPE testing moment is as follows:

$$\begin{aligned}
D_a^1 &= S[2, 0.5, 2.2, 0.7] \\
&= 0.7779 \left[1 + 0.168 \frac{\Lambda_{1S}}{m_Y/2} + 0.345 \left(\frac{\Lambda_{1S}}{m_Y/2} \right)^2 + 0.501 \left(\frac{\Lambda_{1S}}{m_Y/2} \right)^3 + 0.01 \frac{\lambda_1}{(m_Y/2)^2} - 1.05 \frac{\lambda_2}{(m_Y/2)^2} - 1.94 \frac{\lambda_1 \Lambda_{1S}}{(m_Y/2)^3} \right. \\
&\quad - 8.75 \frac{\lambda_2 \Lambda_{1S}}{(m_Y/2)^3} + 6.18 \frac{\rho_1}{(m_Y/2)^3} - 0.25 \frac{\rho_2}{(m_Y/2)^3} + 0.27 \frac{\tau_1}{(m_Y/2)^3} + 3.71 \frac{\tau_2}{(m_Y/2)^3} - 1.50 \frac{\tau_3}{(m_Y/2)^3} \\
&\quad \left. - 1.61 \frac{\tau_4}{(m_Y/2)^3} - 0.0094\epsilon - 0.008\epsilon \frac{\Lambda_{1S}}{m_Y/2} \right]. \tag{39}
\end{aligned}$$

Varying the unknown parameters in the same way, and treating the leading order nonperturbative parameters as unknowns and varying them over the region $\Lambda_{1S} = -0.13 \pm 0.1$ GeV, $\lambda_1 = -0.3 \pm 0.3$ GeV², this moment is predicted to be

$$D_a^1 = 0.7686 \pm 0.0018\epsilon \pm 0.0040_{\text{N.P.}} \tag{40}$$

The perturbative error is obtained by the scale variation in the standard way. As in the lepton spectra, the OPE testing moments are such that with no nonperturbative input other than the known value of λ_2 , we can predict the value of a moment to an accuracy of 1%. As the error on the nonperturbative terms is reduced with global fits, it is important to cross-check with the predicted and measured values of these moments

in order to ensure the error on $|V_{cb}|$ and m_b^{1S} is not being underestimated. Tables V and VI present a selection of OPE testing moments in the parameter space examined.

3. Moments to measure m_b^{1S} with minimal error

Moments that allow a direct measurement of the b quark mass with minimal dependence on the unknown λ_1 nonperturbative parameter have also been found. Moments of this type are important as a measurement of m_b^{1S} to this precision will be an important step in reducing the error on $|V_{ub}|$ as well as extracting $|V_{cb}|$. These moments are particularly suited to being used in a fit to extract the 1S mass. An example of this type of moment is

TABLE VII. The nonperturbative parameters of moments to measure the 1S mass accurately. In the table above the moments are defined in the following way: $B_a^1 = S[3, 0.5, 0.5, 0.9]$, $B_b^2 = S[2.4, 0.5, 1.2, 1.3]$, $B_c^3 = S[2.5, 0.5, 1, 1]$ and $B_d^4 = S[2, 0.5, 1.3, 1.3]$.

	Λ_{1S}	Λ_{1S}^2	Λ_{1S}^3	λ_1	λ_2	$\lambda_1 \Lambda_{1S}$	$\lambda_2 \Lambda_{1S}$	ρ_1	ρ_2	τ_1	τ_2	τ_3	τ_4	
B_a^1	51.9318	35.300	6.06	-1.09	0.93	8.51	3.01	22.32	-13.63	2.01	0.00	-14.30	6.51	5.22
B_b^2	10.2470	4.850	1.38	0.37	0.02	1.74	0.43	3.25	-2.84	-0.03	-0.04	-2.03	0.88	0.72
B_c^3	12.2674	6.116	1.48	0.28	0.31	1.35	0.79	3.62	-3.50	0.24	0.00	-2.43	1.10	0.88
B_d^4	4.7852	1.659	0.55	0.20	0.10	0.55	0.16	0.93	-0.95	-0.11	0.01	-0.62	0.30	0.23

TABLE VIII. The perturbative parameters of moments to measure the 1S mass accurately, and the error estimated in using the moment to extract the 1S mass.

	1S α_s^2 Term		α_s Term		Combined $O(\epsilon)$		Error in extraction of 1S mass
	ϵ	$\Lambda_{1S} \epsilon$	ϵ	$\Lambda_{1S} \epsilon$	ϵ	$\Lambda_{1S} \epsilon$	
B_a^1	-0.003	2.231	4.345	-0.536	4.343	1.70	$\pm 3 \text{ MeV } \epsilon \pm 50 \text{ MeV(N.P.)}$
B_b^2	0.042	0.353	0.383	-0.336	0.426	0.017	$\pm 5 \text{ MeV } \epsilon \pm 55 \text{ MeV(N.P.)}$
B_c^3	0.042	0.454	0.564	-0.318	0.606	0.137	$\pm 1 \text{ MeV } \epsilon \pm 54 \text{ MeV(N.P.)}$
B_d^4	0.017	0.121	0.090	-0.158	0.107	-0.004	$\pm 2 \text{ MeV } \epsilon \pm 59 \text{ MeV(N.P.)}$

$$\begin{aligned}
B_a^1 &= S[3, 0.5, 0.5, 0.9] \\
&= 51.9318 \left[1 + 3.215 \frac{\Lambda_{1S}}{m_Y/2} + 2.609 \left(\frac{\Lambda_{1S}}{m_Y/2} \right)^2 - 2.216 \left(\frac{\Lambda_{1S}}{m_Y/2} \right)^3 + 0.40 \frac{\lambda_1}{(m_Y/2)^2} \right. \\
&\quad + 3.67 \frac{\lambda_2}{(m_Y/2)^2} + 6.14 \frac{\lambda_1 \Lambda_{1S}}{(m_Y/2)^3} + 45.49 \frac{\lambda_2 \Lambda_{1S}}{(m_Y/2)^3} - 27.78 \frac{\rho_1}{(m_Y/2)^3} + 4.10 \frac{\rho_2}{(m_Y/2)^3} \\
&\quad \left. - 0.004 \frac{\tau_1}{(m_Y/2)^3} - 29.15 \frac{\tau_2}{(m_Y/2)^3} + 13.26 \frac{\tau_3}{(m_Y/2)^3} + 10.64 \frac{\tau_4}{(m_Y/2)^3} + 0.084\epsilon + 0.154\epsilon \frac{\Lambda_{1S}}{m_Y/2} \right]. \quad (41)
\end{aligned}$$

Note that moments of this type have a strong dependence on Λ_{1S} and a weak dependence on λ_1 while the coefficients of the higher order terms in the nonperturbative series are not suppressed. These moments are thus well suited to measure the b quark mass with minimal error as the largest source of theoretical error is suppressed in a controlled fashion. Estimating the error on the extraction in the usual way one finds the m_b^{1S} mass extracted from this moment will have a theoretical error of $\pm 50 \text{ MeV(N.P.)} \pm 3 \text{ MeV}(\epsilon)$, where the error is dominated by the unknown nonperturbative corrections at third order. Adding these errors in quadrature one obtains an overall theoretical error in the extraction $\sim 50 \text{ MeV}$. It is important to experimentally measure moments of this type for a precise value of the b quark mass to be extracted from this spectrum. This error assessment in the extraction of m_b^{1S} is assigned in accordance with how the theoretical error is assigned in the OPE testing moments. By measuring both the OPE testing moments and the moments presented in this section, one can extract m_b^{1S} with an experimentally verified theoretical error; comparisons of the b quark mass extracted in this way with extractions using other techniques will be a useful cross-check of theoretical techniques. A selection of moments of this type is given in Tables VII and VIII.

IV. CONCLUSIONS

We have presented the $\mathcal{O}(\alpha_s)$ corrections to the structure functions of the hadronic tensor for $B \rightarrow X_c \ell \bar{\nu}$. The $\mathcal{O}(\alpha_s)$ and $\mathcal{O}(\alpha_s \Lambda_{\text{QCD}}/m_b)$ perturbative corrections for lepton energy moments and hadronic invariant mass moments have been calculated. The effects of the charm quark expansion in fractional moments

was shown to be small and moments that allow one to extract the nonperturbative parameters relevant for a percent level determination of $|V_{cb}|$ from inclusive B decay were presented. Using the techniques outlined, a b quark mass measurement with a theoretical error at the 50 MeV or better should be possible using the inclusive semileptonic decay data. This theoretical error assessment, including the assumption of negligible quark-hadron duality violation that this analysis relies upon, is directly testable with the OPE testing moments presented in this paper. Fits based on the results presented should allow an extraction of $|V_{cb}|$ with $\sim 2\%$ theoretical error. As the lepton energy cut dependence of the $\mathcal{O}(\alpha_s \Lambda_{\text{QCD}}/m_b)$ term is now known, the largest estimated theoretical uncertainty in inclusive extractions of $|V_{cb}|$ and m_b^{1S} comes from the $\mathcal{O}(\alpha_s^2)$ corrections.

ACKNOWLEDGMENTS

It is a pleasure to acknowledge Christian Bauer for collaboration in the early stages of this work, for pointing out the importance of the fractional moment charm quark issues and for comments on the manuscript. I am also grateful to Michael Luke, Craig Burrell and particularly Alex Williamson for helpful discussions and comments on the manuscript. This work was supported in part by the Walter B. Sumner foundation.

APPENDIX A: S_H EXPANSION

The coefficient functions of the general hadronic moment s_H in terms of the pole mass and the HQET local operator expansion are as follows:

$$C_0^0 = 1 + \frac{n\Lambda}{m_b} - \frac{n[\lambda_1 + 3\lambda_2 - (n-1)\Lambda^2]}{2m_b^2} + \frac{(n-1)n\Lambda[(n-2)\Lambda^2 - 3(\lambda_1 + 3\lambda_2)]}{6m_b^3} - \frac{n(\tau_1 + 3\tau_2 + \tau_3 + 3\tau_4 - \rho_1 - 3\rho_2)}{4m_b^3}, \quad (\text{A1})$$

$$C_0^1 = +\frac{\Lambda}{m_b} - \frac{(\lambda_1 + 3\lambda_2 - 2n\Lambda^2)}{2m_b^2} + \frac{n\Lambda[(n-1)\Lambda^2 - 2(\lambda_1 + 3\lambda_2)]}{2m_b^3} - \frac{(\tau_1 + 3\tau_2 + \tau_3 + 3\tau_4 - \rho_1 - 3\rho_2)}{4m_b^3}, \quad (\text{A2})$$

$$C_0^2 = +\frac{\Lambda^2}{2m_b^2} + \frac{\Lambda(n\Lambda^2 - \lambda_1 - 3\lambda_2)}{2m_b^3}, \quad (\text{A3})$$

$$C_0^3 = +\frac{\Lambda^3}{3m_b^3}, \quad (\text{A4})$$

$$C_1^1 = -\frac{\Lambda}{m_b} - \frac{[2(n-1)\Lambda^2 + \lambda_1 + 3\lambda_2]}{2m_b^2} - \frac{(n-1)\Lambda[(n-2)\Lambda^2 - 2(\lambda_1 + 3\lambda_2)]}{2m_b^3} + \frac{(\tau_1 + 3\tau_2 + \tau_3 + 3\tau_4 - \rho_1 - 3\rho_2)}{4m_b^3}, \quad (\text{A5})$$

$$C_1^2 = -\frac{\Lambda^2}{m_b^2} - \frac{2\Lambda[(n-1)\Lambda^2 - \lambda_1 - 3\lambda_2]}{m_b^3}, \quad (\text{A6})$$

$$C_1^3 = -\frac{\Lambda^3}{m_b^3}, \quad (\text{A7})$$

$$C_2^2 = +\frac{\Lambda^2}{m_b^2} + \frac{\Lambda[(n-2)\Lambda^2 - \lambda_1 - 3\lambda_2]}{m_b^3}, \quad (\text{A8})$$

$$C_2^3 = +\frac{\Lambda^3}{m_b^3}, \quad (\text{A9})$$

$$C_3^3 = -\frac{\Lambda^3}{3m_b^3}. \quad (\text{A10})$$

APPENDIX B: HADRONIC INVARIANT MASS MOMENTS FOR FIT

Hadronic moments that are appropriate for a global fit are shown in Tables IX–XIV.

TABLE IX. Coefficients of nonperturbative parameters for $S_{1/2} = S[0.5, E_\ell^{\min}, 0, E_\ell^{\min}]$.

E_ℓ^{\min}	$S_{1/2}^0$	Λ_{1S}	Λ_{1S}^2	Λ_{1S}^3	λ_1	λ_2	$\lambda_1\Lambda_{1S}$	$\lambda_2\Lambda_{1S}$	ρ_1	ρ_2	τ_1	τ_2	τ_3	τ_4
0	2.1799	0.411	0.133	0.07	0.39	-0.05	0.07	0.06	0.35	-0.11	0.10	0.11	0.07	0.03
0.5	2.1771	0.406	0.131	0.07	0.39	-0.04	0.07	0.07	0.35	-0.11	0.10	0.11	0.07	0.03
0.7	2.1735	0.399	0.129	0.07	0.40	-0.03	0.07	0.07	0.35	-0.11	0.10	0.11	0.07	0.04
0.9	2.1685	0.388	0.125	0.07	0.40	-0.01	0.08	0.08	0.37	-0.10	0.10	0.12	0.08	0.04
1.1	2.1625	0.375	0.119	0.06	0.42	0.02	0.09	0.10	0.39	-0.09	0.10	0.13	0.08	0.05
1.3	2.1565	0.362	0.112	0.06	0.44	0.07	0.10	0.12	0.43	-0.08	0.11	0.14	0.08	0.06
1.5	2.1522	0.350	0.104	0.06	0.50	0.12	0.12	0.14	0.51	-0.05	0.12	0.17	0.08	0.07

TABLE X. Coefficients of perturbative parameters for $S_{1/2} = S[0.5, E_\ell^{\min}, 0, E_\ell^{\min}]$.

E_ℓ^{\min}	1S α_s^2 Contribution		α_s Contribution		Combined $O(\epsilon)$	
	ϵ	$\Lambda_{1S} \epsilon$	ϵ	$\Lambda_{1S} \epsilon$	ϵ	$\Lambda_{1S} \epsilon$
0	-0.003	0.023	0.026	0.006	0.023	0.029
0.5	-0.003	0.022	0.031	0.014	0.027	0.037
0.7	-0.003	0.022	0.031	0.017	0.028	0.039
0.9	-0.003	0.021	0.031	0.020	0.027	0.041
1.1	-0.003	0.020	0.030	0.021	0.027	0.041
1.3	-0.004	0.019	0.029	0.023	0.025	0.042
1.5	-0.004	0.018	0.028	0.025	0.024	0.043

TABLE XI. Coefficients of nonperturbative parameters for $S_{3/2} = S[1.5, E_\ell^{\min}, 0, E_\ell^{\min}]$.

E_ℓ^{\min}	$S_{3/2}^0$	Λ_{1S}	Λ_{1S}^2	Λ_{1S}^3	λ_1	λ_2	$\lambda_1 \Lambda_{1S}$	$\lambda_2 \Lambda_{1S}$	ρ_1	ρ_2	τ_1	τ_2	τ_3	τ_4
0	10.286	5.377	1.833	0.56	3.72	-1.00	1.88	0.21	0.63	-0.72	0.76	0.21	0.85	0.50
0.5	10.249	5.296	1.801	0.55	3.77	-0.87	1.90	0.30	0.67	-0.74	0.77	0.24	0.86	0.51
0.7	10.200	5.189	1.757	0.54	3.85	-0.67	1.95	0.42	0.72	-0.77	0.78	0.29	0.87	0.55
0.9	10.133	5.040	1.689	0.53	4.00	-0.35	2.04	0.63	0.81	-0.81	0.81	0.37	0.88	0.60
1.1	10.054	4.859	1.597	0.51	4.25	0.09	2.19	0.92	0.97	-0.84	0.85	0.50	0.91	0.67
1.3	9.976	4.669	1.485	0.48	4.66	0.68	2.46	1.32	1.22	-0.84	0.92	0.72	0.94	0.76
1.5	9.919	4.515	1.366	0.44	5.40	1.43	2.96	1.83	1.69	-0.72	1.05	1.10	0.98	0.89

TABLE XII. Coefficients of perturbative parameters for $S_{3/2} = S[1.5, E_\ell^{\min}, 0, E_\ell^{\min}]$.

E_ℓ^{\min}	1S α_s^2 Contribution		α_s Contribution		Combined $O(\epsilon)$	
	ϵ	$\Lambda_{1S} \epsilon$	ϵ	$\Lambda_{1S} \epsilon$	ϵ	$\Lambda_{1S} \epsilon$
0	-0.041	0.264	0.603	0.402	0.562	0.667
0.5	-0.041	0.261	0.483	0.225	0.443	0.485
0.7	-0.041	0.255	0.458	0.215	0.417	0.470
0.9	-0.041	0.248	0.432	0.216	0.391	0.464
1.1	-0.042	0.239	0.405	0.222	0.363	0.462
1.3	-0.045	0.229	0.380	0.236	0.335	0.465
1.5	-0.053	0.215	0.363	0.263	0.310	0.478

TABLE XIII. Coefficients of nonperturbative parameters for $S_{2a} = S[2, E_\ell^{\min}, 0, E_\ell^{\min}]$.

E_ℓ^{\min}	S_{2a}^0	Λ_{1S}	Λ_{1S}^2	Λ_{1S}^3	λ_1	λ_2	$\lambda_1 \Lambda_{1S}$	$\lambda_2 \Lambda_{1S}$	ρ_1	ρ_2	τ_1	τ_2	τ_3	τ_4
0	22.297	15.253	5.984	1.66	7.93	-1.88	5.00	1.62	-0.89	-1.12	1.47	-0.89	2.23	1.41
0.5	22.189	15.00	5.856	1.64	8.11	-1.50	5.10	1.89	-0.86	-1.25	1.50	-0.79	2.25	1.47
0.7	22.048	14.675	5.685	1.60	8.39	-0.94	5.28	2.28	-0.80	-1.41	1.55	-0.63	2.28	1.55
0.9	21.857	14.222	5.438	1.54	8.88	-0.06	5.60	2.91	-0.69	-1.63	1.63	-0.38	2.32	1.68
1.1	21.634	13.684	5.120	1.46	9.65	1.18	6.13	3.82	-0.50	-1.87	1.76	0.01	2.38	1.87
1.3	21.413	13.122	4.749	1.36	10.90	2.82	7.04	5.03	-0.16	-2.05	1.97	0.63	2.46	2.12
1.5	21.252	12.671	4.378	1.24	13.07	4.93	8.69	6.61	0.48	-2.00	2.30	1.64	2.57	2.44

TABLE XIV. Coefficients of perturbative parameters for $S_{2a}(E_0)$.

E_ℓ^{\min}	1S α_s^2 Contribution		α_s Contribution		Combined $O(\epsilon)$	
	ϵ	$\Lambda_{1S} \epsilon$	ϵ	$\Lambda_{1S} \epsilon$	ϵ	$\Lambda_{1S} \epsilon$
0	-0.104	0.689	1.929	1.367	1.826	2.045
0.5	-0.103	0.679	1.425	0.596	1.321	1.275
0.7	-0.103	0.666	1.322	0.536	1.220	1.202
0.9	-0.104	0.647	1.227	0.526	1.124	1.173
1.1	-0.107	0.624	1.135	0.541	1.028	1.164
1.3	-0.115	0.596	1.051	0.578	0.937	1.174
1.5	-0.135	0.561	0.995	0.656	0.860	1.217

APPENDIX C: LEPTON ENERGY MOMENTS FOR FIT

Lepton energy moments appropriate for extracting Λ_{1S} and $\lambda 1$ from previous work [20] in terms of the inverse upslon mass expansion and $\bar{\Lambda}_{1S} \equiv m_\gamma/2 - m_b^{1S}$ definition of Eq. (22) via $\Lambda_{1S}^{\text{lepton}} = (\bar{m}_B - m_\gamma/2) + \Lambda_{1S}$ are given in Tables XV–XXIII. The general moment is defined for the lepton spectrum in an identical fashion to the general moment for the hadronic invariant mass spectrum.

$$R[n, E_{\ell_1}, m, E_{\ell_2}] = \frac{\int_{E_{\ell_1}}^{E_{\ell_1}^{\max}} E_\ell^n \frac{d\Gamma}{dE_\ell} dE_\ell}{\int_{E_{\ell_2}}^{E_{\ell_1}^{\max}} \hat{E}_\ell^m \frac{d\Gamma}{dE_\ell} dE_\ell}, \quad (\text{C1})$$

TABLE XV. Coefficients of the nonperturbative parameters for $R_1 = R[1, E_\ell^{\min}, 0, E_\ell^{\min}]$.

E_ℓ^{\min}	R_1^0	Λ_{1S}	Λ_{1S}^2	Λ_{1S}^3	λ_1	λ_2	$\lambda_1 \Lambda_{1S}$	$\lambda_2 \Lambda_{1S}$	ρ_1	ρ_2	τ_1	τ_2	τ_3	τ_4
0	1.3920	-0.075	-0.02	0.00	-0.10	-0.21	-0.04	-0.05	-0.03	0.01	-0.02	-0.01	-0.03	-0.03
0.5	1.4216	-0.074	-0.02	0.00	-0.10	-0.21	-0.04	-0.05	-0.03	0.01	-0.02	-0.01	-0.03	-0.03
0.7	1.4611	-0.073	-0.02	0.00	-0.10	-0.20	-0.04	-0.05	-0.03	0.01	-0.02	-0.02	-0.03	-0.03
0.9	1.5173	-0.073	-0.02	0.00	-0.10	-0.20	-0.04	-0.05	-0.04	0.01	-0.02	-0.02	-0.03	-0.03
1.1	1.5884	-0.073	-0.02	0.00	-0.10	-0.19	-0.04	-0.05	-0.04	0.00	-0.02	-0.02	-0.02	-0.03
1.3	1.6724	-0.074	-0.02	0.00	-0.10	-0.18	-0.04	-0.05	-0.04	0.00	-0.02	-0.02	-0.02	-0.03
1.5	1.7674	-0.076	-0.02	0.00	-0.11	-0.17	-0.04	-0.05	-0.05	-0.01	-0.02	-0.03	-0.02	-0.03

TABLE XVI. Coefficients of the perturbative parameters for $R_1(E_0)$.

E_ℓ^{\min}	1S α_s^2 $\alpha_s^3 \beta_0$			α_s $\alpha_s^2 \beta_0$			Combined terms		
	ϵ	$\Lambda_{1S} \epsilon$	ϵ_{BLM}^2	ϵ	$\Lambda_{1S} \epsilon$	ϵ_{BLM}^2	ϵ	$\Lambda_{1S} \epsilon$	ϵ_{BLM}^2
0	0.004	0.001	0.006	-0.001	-0.001	-0.002	0.003	0.000	0.003
0.5	0.004	0.001	0.006	-0.001	-0.001	-0.003	0.003	0.000	0.002
0.7	0.004	0.001	0.006	-0.001	-0.001	-0.004	0.002	0.000	0.002
0.9	0.004	0.001	0.006	-0.002	-0.001	-0.005	0.002	0.000	0.001
1.1	0.004	0.001	0.006	-0.002	-0.001	-0.006	0.001	0.000	0.000
1.3	0.004	0.001	0.006	-0.003	-0.001	-0.007	0.001	0.000	-0.001
1.5	0.004	0.001	0.006	-0.003	-0.001	-0.007	0.001	0.000	-0.001

TABLE XVII. Coefficients of the nonperturbative parameters for variance $V_1 = (R[2, E_\ell^{\min}, 0, E_\ell^{\min}] - R[1, E_\ell^{\min}, 0, E_\ell^{\min}]^2)$.

E_ℓ^{\min}	V_1^0	Λ_{1S}	Λ_{1S}^2	Λ_{1S}^3	λ_1	λ_2	$\lambda_1 \Lambda_{1S}$	$\lambda_2 \Lambda_{1S}$	ρ_1	ρ_2	τ_1	τ_2	τ_3	τ_4
0	0.1804	-0.032	0.00	0.00	-0.05	-0.07	-0.01	-0.01	-0.04	-0.01	-0.01	-0.02	-0.01	-0.01
0.5	0.1542	-0.032	0.00	0.00	-0.05	-0.06	-0.01	-0.01	-0.04	-0.01	-0.01	-0.02	-0.01	-0.01
0.7	0.1280	-0.030	0.00	0.00	-0.05	-0.06	-0.01	-0.01	-0.04	-0.01	-0.01	-0.02	-0.01	-0.01
0.9	0.0988	-0.028	0.00	0.00	-0.05	-0.06	-0.01	-0.01	-0.04	-0.01	-0.01	-0.02	-0.01	-0.01
1.1	0.0705	-0.025	0.00	0.00	-0.05	-0.05	-0.01	-0.01	-0.04	-0.01	-0.01	-0.02	-0.01	-0.01
1.3	0.0458	-0.021	0.00	0.00	-0.05	-0.04	-0.01	-0.01	-0.04	-0.01	-0.01	-0.02	-0.01	-0.01
1.5	0.0261	-0.017	0.00	0.00	-0.04	-0.03	-0.01	-0.02	-0.04	-0.01	-0.01	-0.02	-0.01	-0.01

TABLE XVIII. Coefficients for lepton variance perturbative parameters.

E_ℓ^{\min}	1S α_s^2 $\alpha_s^3 \beta_0$			α_s $\alpha_s^2 \beta_0$			Combined terms				
	ϵ	Λ_{1S}	ϵ	ϵ_{BLM}^2	ϵ	Λ_{1S}	ϵ	ϵ_{BLM}^2	ϵ	Λ_{1S}	ϵ
0	0.002	0.000	0.003	-0.002	0.000	-0.002	0.000	0.000	0.000	0.000	0.001
0.5	0.002	0.000	0.003	-0.002	-0.001	-0.001	0.000	0.000	0.000	0.001	0.001
0.7	0.002	0.000	0.003	-0.002	0.000	-0.001	0.000	0.000	0.000	0.000	0.002
0.9	0.001	0.000	0.002	-0.001	0.000	-0.001	0.000	0.000	0.000	0.000	0.002
1.1	0.001	0.000	0.002	-0.001	0.000	-0.001	0.000	0.000	0.000	0.000	0.002
1.3	0.001	0.000	0.002	-0.001	0.000	-0.001	0.000	0.000	0.000	0.000	0.001
1.5	0.001	0.000	0.002	-0.001	0.000	0.000	0.000	0.000	0.000	0.000	0.001

TABLE XIX. Coefficients for the nonperturbative parameters of $V_2 = \langle (R[1, E_\ell^{\min}, 0, E_\ell^{\min}] - \langle R[1, E_\ell^{\min}, 0, E_\ell^{\min}] \rangle)^3 \rangle$.

E_ℓ^{\min}	V_2^0	Λ_{1S}	Λ_{1S}^2	Λ_{1S}^3	λ_1	λ_2	$\lambda_1 \Lambda_{1S}$	$\lambda_2 \Lambda_{1S}$	ρ_1	ρ_2	τ_1	τ_2	τ_3	τ_4
0	-0.0376	0.001	0.002	0.0	-0.01	0.02	0.0	0.01	-0.03	-0.01	0.0	-0.01	0.0	0.0
0.5	-0.0207	0.0	0.002	0.0	-0.01	0.01	0.0	0.0	-0.03	-0.01	0.0	-0.01	0.0	0.0
0.7	-0.0105	0.0	0.001	0.0	-0.01	0.01	0.0	0.0	-0.03	-0.01	0.0	-0.01	0.0	0.0
0.9	-0.0036	-0.002	0.001	0.0	-0.01	0.01	0.0	0.0	-0.03	-0.01	0.0	-0.01	0.0	0.0
1.1	-0.0001	-0.002	0.001	0.0	-0.01	0.0	0.0	0.0	-0.02	-0.01	0.0	-0.01	0.0	0.0
1.3	0.0009	-0.002	0.0	0.0	-0.01	0.0	0.0	0.0	-0.02	-0.01	0.0	-0.01	0.0	0.0
1.5	0.0009	-0.001	0.0	0.0	-0.01	0.0	0.0	0.0	-0.02	0.0	0.0	0.0	0.0	0.0

TABLE XX. Coefficients for the perturbative parameters of V_2 .

E_ℓ^{\min}	1S α_s^2 $\alpha_s^3 \beta_0$			α_s $\alpha_s^2 \beta_0$			Combined contributions				
	ϵ	Λ_{1S}	ϵ	ϵ_{BLM}^2	ϵ	Λ_{1S}	ϵ	ϵ_{BLM}^2	ϵ	Λ_{1S}	ϵ
0	0.000	0.000	0.000	0.000	0.000	0.001	0.000	0.000	0.000	0.001	0.000
0.5	0.000	0.000	0.000	0.000	0.001	0.000	0.000	0.000	0.001	0.000	0.000
0.7	0.000	0.000	0.000	0.000	0.000	0.000	0.000	0.000	0.000	0.000	0.000
0.9	-0.008	0.000	0.000	0.000	0.007	0.001	0.000	0.000	-0.001	0.001	0.000
1.1	-0.007	0.000	0.000	0.000	0.005	0.000	0.000	0.000	-0.002	-0.001	0.000
1.3	-0.006	0.000	0.000	0.000	0.005	0.000	0.000	0.000	-0.001	0.001	0.000
1.5	-0.005	0.000	0.000	0.000	0.003	0.000	0.000	0.000	-0.002	0.000	0.000

TABLE XXI. Coefficients of the nonperturbative parameters of the lepton energy OPE testing moments, where $D_1 = S[0.2, 1.3, 1, 1]$, $D_2 = S[0.8, 1, 0.1, 1.3]$, $D_3 = S[0.7, 1.6, 1.5, 1.5]$, $D_d^4 = S[2.4, 1, 1.9, 0.8]$ and $D_e^5 = S[2.9, 1.4, 2.2, 1.3]$.

	Λ_{1S}	Λ_{1S}^2	Λ_{1S}^3	λ_1	λ_2	$\lambda_1 \Lambda_{1S}$	$\lambda_2 \Lambda_{1S}$	ρ_1	ρ_2	τ_1	τ_2	τ_3	τ_4	
D_1	0.5452	0.001	-0.003	-0.01	0.002	-0.02	0.00	-0.01	0.01	0.01	0.00	0.01	0.01	0.00
D_2	1.7626	0.014	0.014	0.00	0.001	0.09	0.01	0.05	-0.01	-0.02	0.00	-0.01	0.01	0.01
D_3	0.5215	-0.011	-0.009	0.00	-0.002	-0.04	-0.01	-0.03	0.01	0.01	0.00	0.00	0.00	0.00
D_4	0.6051	-0.015	-0.011	-0.003	-0.006	-0.04	-0.01	-0.03	0.01	0.01	0.00	0.00	0.00	0.00

TABLE XXII. Coefficients of the perturbative parameters of the lepton energy OPE moments.

E_ℓ^{\min}	1S α_s^2 $\alpha_s^3 \beta_0$			α_s $\alpha_s^2 \beta_0$			Combined contributions					
	ϵ	Λ_{1S}	ϵ	ϵ_{BLM}^2	ϵ	Λ_{1S}	ϵ	ϵ_{BLM}^2	ϵ	Λ_{1S}	ϵ	ϵ_{BLM}^2
D_1	0.000	0.000	0.000	0.000	0.000	0.000	0.004	0.001	0.000	0.000	0.000	0.004
D_2	-0.001	0.000	0.000	0.000	-0.001	-0.001	-0.012	-0.002	-0.001	-0.001	-0.001	-0.012
D_3	0.000	0.000	0.000	0.000	0.000	0.000	0.003	0.000	0.000	0.000	0.000	0.003
D_4	0.001	0.001	0.001	0.001	-0.001	-0.001	0.003	0.000	0.000	0.000	0.000	0.004

TABLE XXIII. Predictions and measurements for lepton energy OPE testing moments.

Label	Predicted value	Measured value
D_1	$0.5459 \pm 0.0001\epsilon \pm 0.0010(\text{N.P.})$...
D_2	$1.7585 \pm 0.006\epsilon \pm 0.0036(\text{N.P.})$...
D_3	$0.5200 \pm 0.0001\epsilon \pm 0.0014(\text{N.P.})$	0.5193 ± 0.0008
D_4	$0.6053 \pm 0.0002\epsilon \pm 0.0018(\text{N.P.})$	0.6036 ± 0.0006

- [1] M. A. Shifman and M. B. Voloshin, *Sov. J. Nucl. Phys.* **41**, 120 (1985); J. Chay, H. Georgi, and B. Grinstein, *Phys. Lett. B* **247**, 399 (1990).
- [2] I. I. Bigi *et al.*, *Phys. Lett. B* **293**, 430 (1992); **297**, 477(E) (1993); I. I. Bigi *et al.*, *Phys. Rev. Lett.* **71**, 496 (1993).
- [3] A. V. Manohar and M. B. Wise, *Phys. Rev. D* **49**, 1310 (1994); B. Blok *et al.*, *Phys. Rev. D* **49**, 3356 (1994); **50**, 3572(E) (1994); T. Mannel, *Nucl. Phys.* **B413**, 396 (1994).
- [4] M. B. Voloshin, *Phys. Rev. D* **51**, 4934 (1995).
- [5] M. Gremm and I. Stewart, *Phys. Rev. D* **55**, 1226 (1997).
- [6] M. Gremm, A. Kapustin, Z. Ligeti, and M. B. Wise, *Phys. Rev. Lett.* **77**, 20 (1996).
- [7] A. F. Falk, M. Luke, and M. J. Savage, *Phys. Rev. D* **53**, 2491 (1996).
- [8] A. F. Falk, M. Luke, and M. J. Savage, *Phys. Rev. D* **53**, 6316 (1996).
- [9] M. Gremm and A. Kapustin, *Phys. Rev. D* **55**, 6924 (1997).
- [10] Adam F. Falk, *Nucl. Phys. Proc. Suppl.* **111**, 3 (2002).
- [11] CLEO Collaboration, S. Chen *et al.*, *Phys. Rev. Lett.* **87**, 251807 (2001).
- [12] CLEO Collaboration, D. Cronin-Hennessy *et al.*, *Phys. Rev. Lett.* **87**, 251808 (2001).
- [13] CLEO Collaboration, R. Briere *et al.*, hep-ex/0209024.
- [14] BABAR Collaboration, B. Aubert *et al.*, hep-ex/0207084.
- [15] DELPHI Collaboration, ICHEP Report No. 2002-071-CONF-605, 2002.
- [16] DELPHI Collaboration, ICHEP Report No. 2002-070-CONF-604, 2002.
- [17] C. W. Bauer, Z. Ligeti, M. Luke, and A. V. Manohar, *Phys. Rev. D* **67**, 054012 (2003).
- [18] M. Battaglia *et al.*, *Phys. Lett. B* **556**, 41 (2003).
- [19] I. Gambino and N. Uraltsev, *Eur. Phys. J. C* **34**, 181 (2004).
- [20] C. W. Bauer and M. Trott, *Phys. Rev. D* **67**, 014021 (2003).
- [21] Aida X. El-Khadra and M. Luke, *Annu. Rev. Nucl. Part. Sci.* **52**, 201 (2002).
- [22] A. Hoang, Z. Ligeti, and A. V. Manohar, *Phys. Rev. D* **59**, 074017 (1999).

- [23] A. Hoang, Z. Ligeti, and A.V. Manohar, Phys. Rev. Lett. **82**, 277 (1999); A. H. Hoang and T. Teubner, Phys. Rev. D **60**, 114027 (1999).
- [24] I. I. Bigi, M. A. Shifman, N.G. Uraltsev, and A. I. Vainshtein, Phys. Rev. D **50**, 2234 (1994); M. Beneke and V.M. Braun, Nucl. Phys. **B426**, 301 (1994).
- [25] M. E. Luke, A.V. Manohar, and M. J. Savage, Phys. Rev. D **51**, 4924 (1995).
- [26] M. Jezabek and J. H. Kuhn, Nucl. Phys. **B320**, 20 (1989).
- [27] G. Corbo, Nucl. Phys. **B212**, 99 (1983).
- [28] A. F. Falk, M. Luke, and M. J. Savage, Phys. Rev. D **53**, 2491 (1996).
- [29] F. De Fazio and M. Neubert, J. High Energy Phys. **06** (1999) 017.
- [30] A. Ali and E. Pietarinen, Nucl. Phys. **B154**, 519 (1979).
- [31] Y. Nir, Phys. Lett. B **221**, 184 (1989).
- [32] A. F. Falk and M. Luke, Phys. Rev. D **57**, 424 (1998).
- [33] M. Luke, M. J. Savage, and M. B. Wise, Phys. Lett. B **343**, 329 (1995).
- [34] B. H. Smith and M. B. Voloshin, Phys. Lett. B **340**, 176 (1994).
- [35] I. I. Bigi *et al.*, Phys. Rev. D **52**, 196 (1995).
- [36] M. B. Voloshin, Nucl. Phys. **B154**, 365 (1979).
- [37] H. Leutwyler, Phys. Lett. **98B**, 447 (1981).
- [38] A. Pineda, Nucl. Phys. **B494**, 213 (1997).
- [39] A. I. Vainstein, V. I. Zakharov, and M. A. Shifman, JETP Lett. **27**, 55 (1978); A. A. Shifman *et al.*, Phys. Lett. **77B**, 80 (1978); M. A. Shifman *et al.*, Phys. Lett. **147B**, 385 (1979).
- [40] N. Brambilla, Y. Sumino, and A. Vairo, Phys. Lett. B **513**, 381 (2001).
- [41] M. Beneke and A. Singer, Phys. Lett. B **471**, 233 (1999).
- [42] A. Le Yaouanc *et al.*, Phys. Lett. B **488**, 153 (2000),
- [43] A. Le Yaouanc *et al.*, Phys. Rev. D **62**, 074007 (2000),
- [44] A. Le Yaouanc *et al.*, Phys. Lett. B **517**, 135 (2001).
- [45] I. I. Bigi and N. Uraltsev, Int. J. Mod. Phys. A **16**, 5201 (2001).
- [46] D. Denson, I. I. Bigi, and T. Mannel, Nucl. Phys. **B665**, 367 (2003).
- [47] N. Isgur, Phys. Lett. B **448**, 111 (1999).
- [48] CLEO Collaboration, A. Mahmood *et al.*, Phys. Rev. D **67**, 072001 (2003).
- [49] M. Artuso, hep-ph/0312270.